Superhard nanocrystalline silicon carbide films

Feng Liao and S. L. Girshick[a)]
Department of Mechanical Engineering, University of Minnesota, Minneapolis, Minnesota 55455

W. M. Mook and W. W. Gerberich
Department of Chemical Engineering and Materials Science, University of Minnesota, Minneapolis, Minnesota 55455

M. R. Zachariah
Departments of Mechanical Engineering and Chemistry, University of Maryland, College Park, Maryland 20742

Nanocrystalline silicon carbide films were deposited by thermal plasma chemical vapor deposition, with film growth rates on the order of 10 μm/min. Films were deposited on molybdenum substrates, with substrate temperature ranging from 750-1250 °C. The films are composed primarily of β-SiC nanocrystallites. Film mechanical properties were investigated by nanoindentation. As substrate temperature increased the average grain size, the crystalline fraction in the film, and the hardness all increased. For substrate temperatures above 1200 °C the average grain size equaled 10-20 nm, the crystalline fraction equaled 80-85 %, and the film hardness equaled approximately 50 GPa. © *2005 American Institute of Physics*. [DOI: 10.1063/1.1920434]

Recently there has been a flurry of interest in superhard $Si_xC_y(y \geqslant x)$ materials, where "superhard" is defined to mean hardness $\geqslant 40$ GPa, well above the hardness of standard β-SiC, ~ 28 GPa. Several investigators[1–6] have synthesized SiC-diamond composites using high-pressure, high-temperature powder sintering, and have reported hardnesses ranging from 40-80 GPa. Recently it was reported that hydrogen-free amorphous C-Si films, synthesized by magnetron cosputtering of graphite and silicon, had hardness values of 45-55 GPa for Si mole fractions in the range 38-43 %.[7] However, amorphous SiC films usually contain hydrogen, and have much lower hardness, in the range 10-20 GPa (Ref. 8,9).

Another factor that could potentially result in superhardness is nanocrystallinity. While nanocrystalline SiC is currently of interest for its electronic and optical properties, it has been less studied for its mechanical properties. There are only two prior reports of hardness measurements in nanocrystalline SiC. The first, for bulk-sintered compacts produced from SiC powder, reported results for grain sizes down only to about 70 nm, and the measured hardness did not exceed 27 GPa (Ref. 10). The second, SiC films deposited by hypersonic plasma particle deposition, with grain sizes around 20 nm, measured a peak hardness of 37 GPa (Ref. 11).

We previously reported the deposition of nanocrystalline SiC films by thermal plasma chemical vapor deposition (TPCVD) (Ref. 12). Deposition rates were extremely high, in some cases exceeding 10 μm/min over molybdenum substrates measuring either 19 or 38 mm in diameter. We report here measurements of mechanical properties of these films, several of which were found to have hardness values in the superhard range, up to about 50 GPa. This result does not appear to be attributable to either of the two factors discussed above: there is no evidence of a diamond phase, and, while

some amorphous material may be present, the films are primarily crystalline.

The deposition apparatus has been previously described.[12] The plasma was generated by a radio-frequency (rf) power supply, operating at 3.3 MHz, coupled to an rf induction torch (a modified Tekna PL-35) mounted to a custom-designed CVD chamber. For the experiments reported here the deposition chamber pressure equaled 33.3 kPa, while the rf generator plate power ranged from 15 to 21 kW. The input gases were argon, at a flow rate of 42.5-60 slm; H_2, 0.5-2.5 slm; $SiCl_4$, 68-140 sccm; and methane, at 1.0-1.2 times the $SiCl_4$ flow rate. Molybdenum substrates measuring 19 mm in diameter were mounted in the center of the water-cooled backwall of the CVD chamber. Substrate temperature, which ranged from 750 to 1250 °C (deposition surface), was controlled using a previously described system.[13] Film deposition times ranged from 7 to 15 mins. Film growth rates ranged from 4.1 to 14.9 μm/min^{-1} as determined by micrometer measurement of the film thickness. This somewhat overstates the "true" growth rate, as the films are rough. Scanning electron microscopy images show that
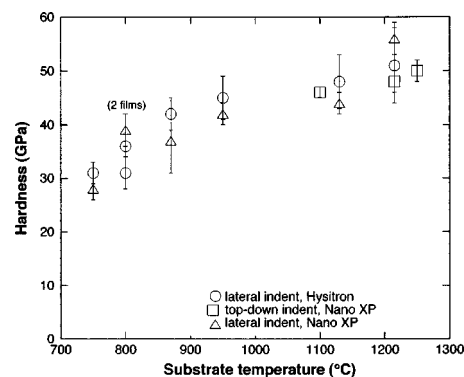

FIG. 1. Film hardness vs substrate temperature during deposition, measured using either the Hysitron Triboscope or the MTS Nano XP nanoindenter, as indicated.
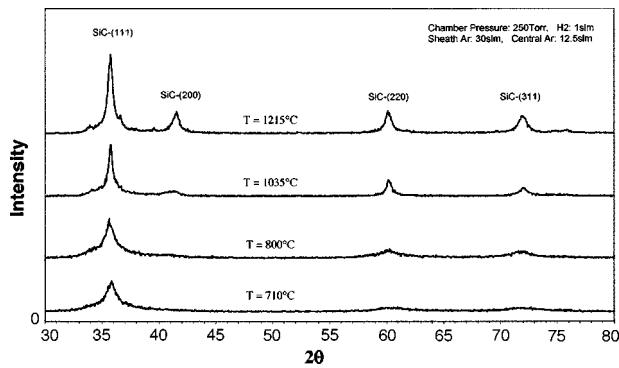
[a)]Electronic mail: slg@tc.umn.edu

FIG. 2. X-ray diffraction spectra for films deposited at different substrate temperatures.

FIG. 3. Average crystallite size and crystalline fraction vs substrate temperature.

the surfaces are partially covered with ball-like hemispheres whose height approximately equals the underlying film thickness.

Two nanoindenter instruments, a Hysitron TriboIndenter and an MTS Nano Indenter-XP, were used to determine film hardness and elastic modulus. The Hysitron instrument was used for indentation loads from 1 to 10 mN, while the MTS instrument was used for indentation loads from 10 to 300 mN.

A major assumption when analyzing load-displacement data generated by nanoindentation is that the film surface is flat. As these films were rough, they needed to be polished to obtain repeatable nanoindentation results. Films were polished and indented both along their cross section and in standard top-down geometries. To polish film cross sections the substrates were sectioned with a diamond saw after deposition. The sample was then mounted in epoxy and polished using standard metallography procedures, utilizing SiC sandpaper (300, 400, and 600 grit), followed by progressively smaller diamond slurries of 9, 3, 1, and 0.25 μm diam. Between each step the samples were sonicated in water. For polishing the films' top surfaces the substrates were mounted in a holder and polished as described above.

The Hysitron data were analyzed using the Oliver and Pharr technique,[14] which infers a single value for hardness and modulus for each load-displacement trace. All of the Hysitron data points in the figures below represent an average over at least ten indentations in different locations, with error bars representing one standard deviation. Data obtained with the MTS instrument were analyzed using the continuous stiffness measurement method,[15] which generates many values of hardness and modulus per each load-displacement trace.

Figure 1 shows measured hardness values versus substrate temperature. Other operating conditions varied for these experiments, according to the ranges noted above, except that the hydrogen flow rate in all cases equaled 1.0 slm. Regardless of the variation in other deposition conditions, a clear trend is observed with regard to substrate temperature. At 750 °C the hardness measured ~30 GPa, approximately equal to the value for standard SiC. As substrate temperature increased the measured hardness increased, reaching about 40 GPa for a substrate temperature of 870 °C, and about 50 GPa for substrate temperatures above 1200 °C. The measured modulus of the films varied linearly with the hardness, ranging from ~265 to ~515 GPa.

Measured film hardness can potentially be affected by residual stresses in the film. Given the relatively small mis-

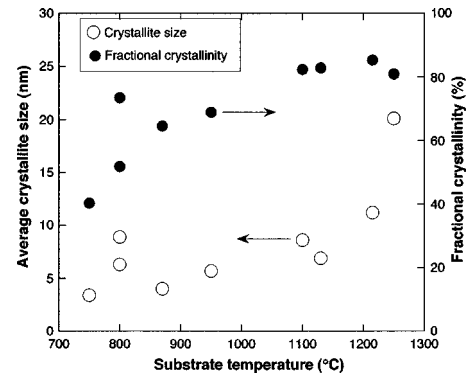match in the thermal expansion coefficient between SiC and Mo, we estimate an upper bound for residual stresses in these films of ~0.25 GPa. This level of residual stress would be expected to have little effect on the very large hardnesses and moduli that we measured, especially as most of the measurements were made with indentations of the film cross section (labeled "lateral indent" in Fig. 1), whereas the residual stress, if it exists, would act in the direction parallel to the film substrate.

A number of factors could potentially explain the increase in hardness observed with increasing substrate temperature. For example, higher substrate temperatures could promote the appearance of a diamond or sp^3-bonded carbon phase, or could otherwise affect the crystalline phase composition, or the grain size and density.

Figure 2 shows x-ray diffraction (XRD) spectra for four films deposited at different substrate temperatures. XRD spectra for all films were dominated by the β-SiC (111) peak at $2\theta = 35.6°$. As substrate temperature increased several other β-SiC peaks became gradually more pronounced, and the peak at 35.6° developed shoulders associated with α-SiC. However, no XRD peaks associated with diamond were observed.

The elemental composition in the films was measured with Rutherford backscattering spectrometry (RBS), using 3.7-MeV He ions with a commercial SiC wafer as reference. For all but two of the films included in Fig. 1 the C/Si ratio was within 3% of stoichiometric SiC, and both of the films that lay outside that range were deposited at 800 °C, and had hardness below 40 GPa. Thus, the superhard films did not contain excess carbon, as would be required for a SiC-diamond composite.

Raman spectroscopy measurements were obtained for two films, including the superhard film deposited at 1215 °C. These measurements were performed using excitation at 514.5 and 1064 nm (Fourier-transform Raman spectroscopy). While Raman spectra of nanocrystalline SiC are complex and not yet well understood, it can at least be stated that the spectra for the two films measured show SiC and other features, tentatively ascribed to silicon and sp^2 carbon, but do not show the 1332-cm^{-1} peak characteristic of diamond.[16]

If diamond is not present, another possible explanation for the emergence of superhardness at elevated substrate temperatures is the appearance in XRD spectra, for substrate temperatures above about 1100 °C, of the peak associated with β-SiC-(200). In a recent theoretical study of β-SiC surface energies, a negative surface energy of −0.4 to −0.49 eV/atom for the [100] surface was reported, compared
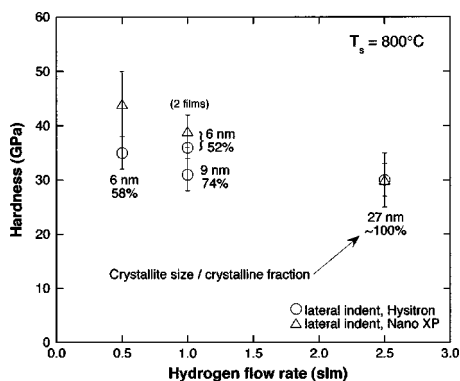
FIG. 4. Measured hardness vs hydrogen flow rate, for films deposited at a substrate temperature of 800 °C.

to 0.35–1.15 eV/atom for the [111] surfaces, the ranges depending on the various types of surface terminations.[17] Thus the (200) peak found in our study suggests an unstable surface capable of reconstruction at high temperature. This metastable microstructure may enhance densification at high substrate temperatures, thus leading to superior properties.

Figure 3 shows the effect of substrate temperature on average crystallite size and fractional crystallinity, for the same films whose hardness is shown in Fig. 1. Average crystallite size was determined by Fourier analysis of the XRD spectra based on the Warren-Averbach method,[18–20] using the software WINFIT (Ref. 21). Crystalline fraction was calculated from the XRD spectra using the software JADE (Materials Data, Inc.). It should be noted that, in addition to amorphous SiC at grain boundaries, the "noncrystalline" fraction in this evaluation may include SiC crystallites smaller than 1-2 nm and SiC with stacking faults.

Both crystallite size and crystalline fraction increased along with substrate temperature. Average crystallite size for these films ranged from 3.4 to 20.1 nm, while crystalline fraction ranged from 40% to 85%. Given that substrate temperature affects both grain size and crystalline fraction it is difficult to draw conclusions regarding the effect of grain size on hardness. The films with hardness around 50 GPa have average grain sizes in the 10-20 nm range and crystalline fractions of 80-85 %.

To further investigate the relation between film hardness and crystallinity we measured the hardness of four films that were deposited at the same substrate temperature, 800 °C, but at various hydrogen flow rates, ranging from 0.5 to 2.5 slm. For three of these films all deposition conditions other than the hydrogen flow rate were identical. For the fourth film (the harder of the two films in Fig. 4 for which the hydrogen flow rate equaled 1.0 slm) several other conditions differed.

Figure 4 shows the measured hardness as well as the average crystallite sizes and crystalline fractions in these films. The results for crystallinity are consistent with previous observations that hydrogen promotes crystallization in SiC (Refs. 22,23). At a hydrogen flow rate of 2.5 slm the film is fully crystalline, with an average grain size of 27 nm, but the hardness, ~30 GPa, is approximately equal to that of standard SiC. At lower hydrogen flow rates the crystalline fraction was smaller, as was the grain size, while the hardness increased. A reasonable hypothesis is that increasing the hydrogen flow rate, while it promotes crystallization, also increases the hydrogen content in the noncrystalline phase.

In view of the discovery that amorphous SiC can be super-hard if free of hydrogen,[7] these results suggest that hardness in these films is determined by a combination of nanocrystallite size, crystalline fraction, and the composition of the amorphous phase that lies at grain boundaries.

Finally, the fracture toughness of four of the films, deposited at substrate temperatures ranging from 800 to 1250 °C was determined by indenting the polished top surface with a Vickers diamond tip using loads high enough so that cracks develop from the corners of the indent. The measured fracture toughness of these films ranged from 3.9 to 4.8 MPa m$^{1/2}$, which is higher than reported values[24–26] for β-SiC of 2.8–3.3 MPa m$^{1/2}$.

[1]O. O. Mykhaylyk and M. P. Gadzira, Acta Crystallogr., Sect. B: Struct. Sci. **55**, 297 (1999).
[2]E. A. Ekimova, A. G. Gavriliuk, B. Palosz, S. Gierlotka, E. Tatianin, Y. Kluev, A. M. Naletov, and A. Presz, Appl. Phys. Lett. **77**, 954 (2000).
[3]O. O. Mykhaylyka and M. P. Gadzira, J. Mater. Chem. **11**, 217 (2001).
[4]Y. S. Ko, T. Tsurumi, O. Fukunaga, and T. Yano, J. Mater. Sci. **36**, 469 (2001).
[5]J. Qian, G. Voronin, T. W. Zerda, D. He, and Y. Zhao, J. Mater. Res. **17**, 2153 (2002).
[6]Y. Zhao, J. Qian, L. L. Daemen, C. Pantea, J. Zhang, G. A. Voronin, and T. W. Zerda, Appl. Phys. Lett. **84**, 1356 (2004).
[7]V. Kulikovsky, V. Vorlícek, P. Bohác, A. Kurdyumov, and L. Jastrabík, Diamond Relat. Mater. **13**, 1350 (2004).
[8]J. F. Zhao, P. Lemoine, Z. H. Liu, J. P. Quinn, P. Maguire, and J. A. McLaughlin, Diamond Relat. Mater. **10**, 1070 (2001).
[9]P. Papakonstantinou, J. F. Zhao, P. Lemoine, E. T. McAdams, and J. A. McLaughlin, Diamond Relat. Mater. **11**, 1074 (2002).
[10]R. Vassen and D. Stöver, J. Am. Ceram. Soc. **82**, 2585 (1999).
[11]N. Tymiak, D. I. Iordanoglou, D. Neumann, A. Gidwani, F. Di Fonzo, M. H. Fan, N. P. Rao, W. W. Gerberich, P. H. McMurry, J. V. R. Heberlein, and S. L. Girshick, in *Proceedings of the 14th International Symposium on Plasma Chemistry*, Prague, 2-6 August 1999, edited by M. Hrabovský, M. Konrád, and K. Kopecký (Institute of Plasma Physics, Academy of Sciences of the Czech Republic), Vol. 3, p. 1989.
[12]F. Liao, S. Park, J. M. Larson, M. R. Zachariah, and S. L. Girshick, Mater. Lett. **57**, 1982 (2003).
[13]M. T. Bieberich and S. L. Girshick, Plasma Chem. Plasma Process. **16**, 157S (1996).
[14]W. C. Oliver and G. M. Pharr, J. Mater. Res. **7**, 297 (1992).
[15]W. C. Oliver and J. B. Pethica, U.S. Patent No. 4,848,141 (18 July 1989).
[16]D. S. Knight and W. B. White, J. Mater. Res. **4**, 385 (1989).
[17]Z. Lodziana, N.-Y. Topsoe, and J. K. Norskov, Nat. Mater. **3**, 289 (2004).
[18]B. E. Warren and B. L. Averbach, J. Appl. Phys. **21**, 595 (1950).
[19]D. D. Eberl and A. Blum, in *Computer Applications to X-Ray Powder Diffraction Analysis of Clay Minerals*, Clay Minerals Society Workshop Lectures, edited by R. C. Reynolds and J. R. Walker (Clay Minerals Society, Boulder, Colorado, 1993), Vol. 5, p. 123.
[20]C. N. J. Wagner and E. N. Aqua, Adv. X-Ray Anal. **7**, 46 (1964).
[21]S. Krumm, Mater. Sci. Forum **228-231**, 183 (1996) in *Proceedings of the European Diffraction Conference*, Chester, England, July 1995, edited by R. J. Cernik, R. Delhez, and E. J. Mittemeijer.
[22]S. Kerdiles, R. Rizk, F. Gourbilleau, A. Pérez-Rodríguez, B. Garrido, O. González-Varona, and J. R. Morante, Mater. Sci. Eng., B **B69-70**, 530 (2000).
[23]Q. Zhao, J. C. Li, H. Zhou, H. Wang, B. Wang, and H. Yan, J. Cryst. Growth **260**, 176 (2004).
[24]M. J. Slavin and G. D. Quinn, Int. J. High Technol. Ceram. **2**, 47 (1986).
[25]Morgan Advanced Ceramics (http://www.performancematerial.com/sic_physical.htm)
[26]Rohm and Haas Company (http://www.cvdmaterials.com/sicprop1.htm)